New treatment of strongly anisotropic scattering phase functions: The Delta-M+ method

Zhenyi Lin*, Nan Chen, Yongzhen Fan, Wei Li, and Knut Stamnes

Department of Physics & Engineering Physics, Stevens Institute of Technology, Hoboken, NJ, USA

Snorre Stamnes

NASA Langley Research Center, Hampton, VA, USA

Corresponding author address: Zhenyi Lin, Department of physics & Engineering physics,

Stevens Institute of Technology

E-mail: lzhenyi@stevens.edu

1

ABSTRACT

The treatment of strongly anisotropic scattering phase functions is still a challenge for accurate radiance computations. The new Delta-M+ method resolves this problem by introducing a reliable, fast, accurate, and easy-to-use Legendre expansion of the scattering phase function with modified moments. Delta-M+ is an upgrade of the widely-used Delta-M method that truncates the forward scattering peak with a Dirac delta function, where the '+' symbol indicates that it essentially matches moments beyond the first M terms. Compared with the original Delta-M method, Delta-M+ has the same computational efficiency, but for radiance computations the accuracy and stability have been increased dramatically.

1. Introduction

In most current scalar radiative transfer models for radiance computations in plane parallel geometry (Stamnes et al., 1988, 2000; Jin et al., 2006; Spurr, 2008; Rozanov et al., 2014; Lin et al., 2015; Stamnes and Stamnes, 2016; Hamre et al., 2017; Stamnes et al., 2017a), the scattering phase function is expanded in a finite series of Legendre polynomials. This expansion of the scattering phase function combined with an expansion of the radiance in a Fourier cosine series leads to a radiative transfer equation (RTE) for each Fourier component that is azimuth-independent and mathematically identical for all Fourier components (Stamnes et al., 1988). As a result, an accurate and stable RTE solution relies on an adequate expansion of the scattering phase function, which could be computationally expensive, because a strongly asymmetric scattering phase function may require hundreds of terms in a standard Legendre polynomial expansion. For example, Kokhanovsky et al. (2010) used 480 terms to expand a scattering phase function for a polydispersion of aerosol particles and 720 terms for a polydispersion of (water) cloud droplets in order to produce accurate radiative transfer benchmark results.

In order to alleviate the computational burden, truncation methods (Joseph et al., 1976; Wiscombe, 1977; Nakajima and Tanaka, 1988; Hu et al., 2000; Mitrescu and Stephens, 2004) have been introduced in which the required number of terms in the expansion is reduced by replacing the sharp forward scattering peak by a Dirac delta function. Two popular truncation methods are the δ-M (Wiscombe, 1977) and the δ-fit (Hu et al., 2000) methods. Overall, combined with the single-scattering correction (Nakajima and Tanaka, 1988), the δ-M method, in comparison with other truncations methods, was shown to provide the most accurate radiances for scattering phase functions that are not too strongly forward-peaked (Rozanov and Lyapustin, 2010). The δ-M algo-

$_{43}$ rithm is implemented in many radiative transfer models including DISORT (Stamnes et al., 1988)

$_{44}$ used in MODTRAN (Berk et al., 2014).

$_{45}$ Nevertheless, none of the current truncation methods is perfect (Rozanov and Lyapustin, 2010).

$_{46}$ The δ-M method, designed for irradiance calculations, was found to be unable to provide accurate

$_{47}$ radiances for strongly anisotropic scattering. The δ-fit method can provide accurate radiances

$_{48}$ (except in the forward direction), but requires an *ad hoc* specification of the truncation angle

$_{49}$ and a higher computational burden than δ-M. A δ-fit user must specify by trial and error the

$_{50}$ "best" truncation angle for each scattering phase function, and the least squares fitting employed

$_{51}$ in the δ-fit method also implies additional computations. These problems make the δ-fit method

$_{52}$ inconvenient to use and slower than the δ-M method.

$_{53}$ In this paper, we will address these issues by introducing a new truncation technique, the δ-M+

$_{54}$ method, designed for efficient yet accurate computation of radiances in turbid media with strongly

$_{55}$ asymmetric scattering phase functions. The new δ-M+ method represents an extension and up-

$_{56}$ grade of the standard δ-M algorithm, which leads to a significant improvement in accuracy, while

$_{57}$ retaining the same computational efficiency and "user-friendliness" as the original δ-M method

$_{58}$ (Wiscombe, 1977).

$_{59}$ ## 2. Review of the Delta-M method

$_{60}$ In a full-range slab geometry the radiative transfer equation for the diffuse radiance may be

$_{61}$ written as (Stamnes et al., 2017a)

$$u\frac{dI(\tau,u,\phi)}{d\tau} = I(\tau,u,\phi) - \frac{\varpi}{4\pi}\int_0^{2\pi}d\phi'\int_{-1}^{1}du'p(u',\phi';u,\phi)I(\tau,u',\phi')$$
$$- (1-\varpi)B - S^*(\tau,u,\phi), \tag{1}$$

4

where τ is the optical depth, u is the cosine of the polar angle θ, ϕ is the relative azimuth angle, ϖ is the single-scattering albedo, and $p(u',\phi';u,\phi)$ is the scattering phase function. The term $S^*(\tau,u,\phi)$, proportional to the incident solar beam irradiance F^s, is given by

$$S^*(\tau,u,\phi) = \frac{\varpi}{4\pi} p(u',\phi';u,\phi) F^s e^{-\tau/\mu_0} \tag{2}$$

where μ_0 is the cosine of the incident (solar) zenith angle. To obtain the radiance, we have to solve for a function of *three* variables, τ, u, and ϕ. But this three-variable problem can be reduced to one of solving a finite set of uncoupled radiative transfer equations, each depending on only the two variables τ and u. We start by expanding the scattering phase function in a finite series of M *Legendre polynomials* as follows ($\cos\Theta = uu' + \sqrt{1-u^2}\sqrt{1-u'^2}\cos(\phi-\phi')$):

$$p(\cos\Theta) = p(u',\phi';u,\phi) \approx \sum_{\ell=0}^{M-1} (2\ell+1)\chi_\ell P_\ell(\cos\Theta), \tag{3}$$

where P_ℓ is the ℓth *Legendre polynomial*, and the ℓth expansion coefficient is given by:

$$\chi_\ell = \frac{1}{2}\int_{-1}^{1} d(\cos\Theta)P_\ell(\cos\Theta)p(\cos\Theta). \tag{4}$$

To simplify the expansion of the scattering phase function we use the *Addition Theorem for Spherical Harmonics* (Arfken and Weber, 1999):

$$P_\ell(\cos\Theta) = P_\ell(u')P_\ell(u) + 2\sum_{m=1}^{\ell} \Lambda_\ell^m(u')\Lambda_\ell^m(u)\cos m(\phi'-\phi) \tag{5}$$

where we have introduced the *normalized associated Legendre polynomial* defined by

$$\Lambda_\ell^m(u) \equiv \sqrt{\frac{(\ell-m)!}{(\ell+m)!}}P_\ell^m(u), \tag{6}$$

where $P_\ell^m(u)$ is the *associated Legendre polynomial*.

In the δ-M method, we introduce an approximate scattering phase function $p^*(\cos\Theta)$ (Wiscombe, 1977):

$$p^*(\cos\Theta) = 2f\delta(1-\cos\Theta) + (1-f)\sum_{\ell=0}^{M-1}(2\ell+1)\chi_\ell^* P_\ell(\cos\Theta) \tag{7}$$

5

where the first term is the Dirac δ function and f is the truncation factor. The second term on the right is called the "truncated scattering phase function", whose coefficients χ_ℓ^* are determined by matching them to the χ_ℓ of the accurate (true) scattering phase function, given by Eq. (4). This requirement leads to

$$\chi_\ell^* = \frac{\chi_\ell - f}{1 - f}, \quad \ell = 0, \cdots, M - 1 \tag{8}$$

$$f = \chi_M. \tag{9}$$

After the truncation, the radiative transfer equation is unchanged, except that the optical depth τ and the single-scattering albedo ϖ are scaled as follows:

$$d\tau' = (1 - \varpi f)d\tau \tag{10}$$

$$\varpi' = \frac{1 - f}{1 - \varpi f}\varpi \tag{11}$$

where τ' and ϖ' are the scaled variables resulting from using the approximate scattering phase function in Eq. (7).

3. The error of the Delta-M truncation

Due to the orthogonality of the Legendre polynomials, the Dirac delta function in Eq. (7) may be expanded in an infinite series of Legendre polynomials:

$$2f\delta(1 - \cos\Theta) = \sum_{\ell=0}^{\infty}(2\ell + 1)fP_\ell(\cos\Theta). \tag{12}$$

In Eq. (12), a very important feature is the constant coefficient f for all terms in the sum. Substituting Eqs. (8) and (12) into Eq. (7), we find that the approximate scattering phase function becomes:

$$p^*(\cos\Theta) = \sum_{\ell=0}^{M-1}(2\ell + 1)\chi_\ell P_\ell(\cos\Theta) + \sum_{\ell=M}^{\infty}(2\ell + 1)fP_\ell(\cos\Theta). \tag{13}$$

6

We note that the first M terms in Eq. (13) contain the standard Legendre expansion coefficients (or moments) χ_ℓ given by Eq. (4). Hence, the error incurred by applying the approximate scattering phase function is included in the higher order terms with $\ell \geq M$:

$$\varepsilon = p(\cos\Theta) - p^*(\cos\Theta) = \sum_{\ell=M}^{\infty}(2\ell+1)(\chi_\ell - f)P_\ell(\cos\Theta). \tag{14}$$

Figure 1 shows an example of δ-M and δ-M+ moments (Legendre polynomial expansion coefficients) for a H-G scattering phase function approximated by a truncated 20-term ($M = 20$) expansion. We note that the first 20 moments are accurate, but the error for higher order moments ($\ell \geq 20$, shown as $\chi_\ell^* - \chi_\ell$) is much larger in the δ-M approximation than in the δ-M+ approximation.

4. A modified representation of the Dirac delta Function

The δ-M method, which assumes a constant truncation for all Legendre moments, leads to large errors in higher order moments. To overcome this problem, we introduce a weighted Legendre series for the delta function as a new approximation of the Dirac delta function $\delta^*(1-\cos\Theta)$, which we write as:

$$2f\delta^*(1-\cos\Theta) = \sum_{\ell=0}^{\infty}(2\ell+1)w_\ell f P_\ell(\cos\Theta) \tag{15}$$

$$w_\ell = c \cdot \exp\left(-\frac{\ell^2}{2\sigma^2}\right), \qquad \ell = 0, 1, 2, \ldots. \tag{16}$$

In Eq. (15), the coefficients are changed from a constant value f to the weighted values $w_\ell f$. The purpose of introducing weights is to produce a new function that is still sharply peaked and looks close to a delta function, but also, by a suitable choice of the weights, agrees better with the actual scattering phase function for higher order moments ($\ell > M$). For simplicity, we assumed that the weights w_ℓ have a Gaussian distribution as shown in Eq. (16), where the value of c and σ are to be determined by matching $2\delta^*(1-\cos\Theta)$ to the higher order of Legendre moments described in

the next section. Applying the approximate δ function given by Eq. (15), we now introduce a new, improved approximate scattering phase function, given by:

$$p_{\text{new}}^*(\cos\Theta) = 2f\delta^*(1-\cos\Theta) + \sum_{\ell=0}^{M-1}(2\ell+1)(\chi_\ell - w_\ell f)P_\ell(\cos\Theta). \tag{17}$$

Figure 1 shows how moment errors $(\chi_\ell^* - \chi_\ell)$ in higher orders are reduced after using the new approximate scattering phase function (which is labeled as "New δ-M+").

One may ask what would the new approximate function $\delta^*(1-\cos\Theta)$ look like? Figure 2 shows an example of the shape of w_ℓ and the corresponding $\delta^*(1-\cos\Theta)$ for different combinations of c and σ. Looking at Fig. 2, we first realize that the new approximate function is normalized to w_0, which is greater than 1.0. Therefore, it magnifies the truncation factor f in the original δ-M method. This magnification is desired because a larger forward peak truncation is needed to truncate the strongly anisotropic scattering phase function. Second, the shape of the new function just looks like a sharp spike in the forward direction, whose magnitude and width are determined by the parameters σ and c. These two parameters give us more freedom to control the sharp forward scattering peak. Third, as σ increases, the lower order moments of w_ℓ $(\ell = 0, 1, \ldots, M-1)$ become closer to 1, and we see that the new approximate delta function approaches the original delta function (e.g. for $\sigma = 48$ in Fig. 2, $w_\ell \approx 1$, for $\ell = 0, 1, 2, \cdots, 16$). Under this condition, the δ-M+ truncation will approach the original δ-M truncation.

5. The new δ-M+ method

Based on the new approximate Dirac delta function (Eq. (15)), we upgraded δ-M and developed a new δ-M+ truncation method. Since in Wiscombe (1977), M is essentially the order of the approximation ($M = 1$ leads to the delta-two-stream or delta-Eddington approximation), we use

8

the '+' sign to indicate an improved approximation for moments beyond the Mth moment by adjusting the values of the higher order weights.

In general, the ideal way to match higher order moments is to make every higher order term of Legendre moments correct:

$$w_\ell f = \chi_\ell, \qquad \ell = M, \, M+1, \, M+2, \, \ldots \tag{18}$$

However, since it is more important to get correct lower order moments than higher order ones, and since we only have two Gaussian parameters (c and σ) available to control the shape of $\delta^*(1 - \cos\Theta)$, we simply match the $(M)^{\text{th}}$ and $(M+1)^{\text{th}}$ Legendre moments by setting:

$$\begin{cases} w_M f = \chi_M \\[2mm] w_{M+1} f = \chi_{M+1}. \end{cases} \tag{19}$$

Note that we also define $f = \chi_M$ as in the original δ-M method so that $w_M = 1$. The solution of Eq. (19) is straightforward and given by:

$$f = \chi_M \tag{20}$$

$$w_M = 1 \tag{21}$$

$$\sigma = \sqrt{\frac{(M+1)^2 - M^2}{\ln \chi_M^2 - \ln \chi_{M+1}^2}} \tag{22}$$

$$c = w_0 = \exp\left(\frac{M^2}{2\sigma^2}\right). \tag{23}$$

The constant c is determined by the normalization $w_M = 1$, and $c = w_0 > 1$, which could be considered as a magnification factor of f. Next, the truncated scattering phase function in Eq. (17)

9

is normalized by dividing by $(1 - w_0 f) = (1 - f')$:

$$\chi_\ell^* = \frac{\chi_\ell - w_\ell f}{1 - f'} \tag{24}$$

$$= \frac{\chi_\ell - f' \exp\left(-\ell^2/2\sigma^2\right)}{1 - f'}, \quad \ell = 0, 1, 2, \ldots, M-1 \tag{25}$$

$$f' = w_0 f = \exp\left(M^2/2\sigma^2\right) \chi_M \tag{26}$$

where we see that the new truncation factor $f' \geq f$.

At last, we need to scale the optical depth τ and the single-scattering albedo ϖ for the new method in a similar manner as in the δ-M method:

$$d\tau' = (1 - \varpi f')d\tau \tag{27}$$

$$\varpi' = \frac{1 - f'}{1 - \varpi f'}\varpi. \tag{28}$$

6. Examples and comparison of scattering phase functions

a. Henyey-Greenstein scattering phase function

The Legendre polynomial expansion of the Henyey-Greenstein (H-G) scattering phase function (Henyey and Greenstein, 1941) with asymmetry factor g is

$$p_{\text{HG}}(\cos\Theta) \approx \sum_{\ell=0}^{M-1} (2\ell+1)g^\ell P_\ell(\cos\Theta). \tag{29}$$

In Figure 3, three H-G scattering phase functions with asymmetry factor $g = 0.85$ are shown in the left panel: the accurate scattering phase function, δ-M truncated scattering phase function and the new δ-M+ truncated scattering phase function. Sixteen terms were used to expand the truncated scattering phase function. The right panel shows relative errors of the δ-M and the new δ-M+ scattering phase functions.

Except for unavoidable errors around the forward peak, the new δ-M+ scattering phase function looks essentially the same as the actual (true) scattering phase function at other angles, whereas

10

the original δ-M scattering phase function fluctuates around the true scattering phase function,

whose relative error increases with scattering angle Θ.

b. Aerosol scattering phase function

To test the new δ-M+ method for large aerosol particles, we used the scattering phase function

adopted in Kokhanovsky's benchmark paper (Kokhanovsky et al., 2010), where a Mie code was

used to compute the scattering phase function at 412 nm assuming that the radius a of the aerosol

particles follows a lognormal distribution

$$f(a) = \frac{1}{\sqrt{2\pi}sa} \exp(-\ln^2(a/a_0)/2s^2) \tag{30}$$

with $a_0 = 0.2\ \mu$m, $s = 0.92$ and $a_{\text{end}} = 30\ \mu$m. The value of a_{end} specifies the upper limit of

integration of Mie optical cross section with respect to the particle radius a. The lower limit of

integration was equal to $0.005\ \mu$m. The refractive index of the aerosol particles was set to 1.385.

Figure 4 shows the true, the δ-M, and the new δ-M+ scattering phase functions for this aerosol

case. The truncated scattering phase function is expanded using 32 terms. While the δ-M method

has a relative error up to 0.2 (20%), the error has been greatly reduced for the new δ-M+ method.

c. Water cloud scattering phase function

Similar to the aerosol test, the cloud droplet distribution from Kokhanovsky's benchmark is used

for the cloud case (Kokhanovsky et al., 2010). As in the aerosol case, the scattering phase function

was computed by a Mie code based on a narrow lognormal distribution, where $a_0 = 5\ \mu$m, $s = 0.4$,

$a_{\text{end}} = 100\ \mu$m and the refractive index was set to $m_{\text{r}} = 1.339$. The maximum forward peak has a

very large value reaching $7,830$, and there are pronounced rainbow and glory features (two more

peaks). We used 64 terms to expand the truncated scattering phase function. Again a comparison

of relative errors shows that the new δ-M+ method greatly outperforms the old method and gives results with high accuracy (see Fig. 5).

d. Stability test for extreme scattering phase functions

We have already tested the δ-M+ method on large aerosol and water cloud particles, and reduced the relative errors significantly, but we still do not know how well the δ-M+ method automatically truncates extreme anisotropic scattering phase functions.

Two extreme scattering phase functions were introduced here based on the H-G scattering phase function and the Fournier-Forand (FF) scattering phase function (Fournier and Forand, 1994). In the first test we used the H-G scattering phase function with $g = 0.999$, yielding a scattering phase function that is extremely forward-peaked, whose peak magnitude reaches around $2,000,000$. We used only 32 terms to expand the truncated scattering phase function. The results show that new δ-M+ method works very well, while the original δ-M method oscillates strongly and gives negative values (see Fig. 6).

Another sharply peaked scattering phase function is the Fournier-Forand (FF) function. We adopted a refractive index (real part, $m_r = 1.0686$) typical of pigmented (phytoplankton) particles and used 32 terms to test the new δ-M+ method. Again, the new method was found to work well while the original δ-M method failed to converge as shown in Fig. 7.

e. Ice cloud scattering phase function

Finally, we tested the expansion of an ice cloud scattering phase function at 0.55μm (Takano and Liou, 1989). Compared with the water cloud scattering phase function, the scattering phase function of ice crystals is more challenging because it has not only a stronger forward peak (reaching $100,000$), but also halo peaks at other scattering angles which may not necessarily benefit from the

12

truncation of the forward scattering peak. As a result, hundreds of expansion terms are required for accurate expanding those additional peaks even by the δ-M+ method. Applied 100 and 200 expansion terms we obtained the results shown in Fig. 8. We see that the Delta-M+ method has a better truncation of the forward peak than the original Delta-M method, which fails to adequately represent the ice crystal scattering phase function even when using 200 terms.

7. Radiance tests

From Sections 6b and 6c, it is clear that the new δ-M+ method works well and provides accurate representations of the Kokhanovsky aerosol and cloud scattering phase functions. Here, we first revisit these benchmarks to look at the relative error (%) of the reflectance as a function of viewing polar angle. The Kokhanovsky benchmarks assume a homogeneous aerosol/cloud slab and a direct beam incident at $60°$ at the top of the slab. The optical depth of the slab was 0.3262 for the aerosol case and 5.0 for the cloud case, respectively.

In Fig. 9 relative errors of the Kokhanovsky aerosol benchmark results are shown for the original δ-M and the new δ-M+ methods. Generally, we see that the errors have been greatly reduced from 10% to less than 1% for most viewing angles. An exception happens around the exact backward scattering angle ($\Delta\phi = 180°, \theta = 60°$). Considering that the reflectance is very small at the backscattering angle, and that we used only 32 streams to compute the reflectance (instead of 480 in the benchmark), these errors are quite small implying that the new δ-M+ method performs satisfactorily.

Figure 10 shows the relative errors of the Kokhanovsky cloud benchmark results. Once again, the new δ-M+ method greatly reduces the relative error and provides satisfactory results.

Finally, a slab of particles with the extremely forward-peaked FF scattering phase function shown in Fig. 7 is used to test the radiance output. The upward radiances at three azimuth an-

13

221 gles are shown in Fig. 11, where the incident beam angle is $30°$, and the slab optical thickness

222 is set to be 0.5. The results show strong oscillations of the radiances computed with the original

223 δ-M, which could not yield converged results even for 200 streams, while the new δ-M+ method

224 provides smooth and stable results for only 32 streams.

8. Summary and discussion

226   The δ-M+ method is an enhanced version of the δ-M method that maintains the same compu-

227 tational efficiency but improves the accuracy significantly. By applying Gaussian weights $w_\ell f$ to

228 represent the truncation peak, the new δ-M+ method eliminates the errors of the Legendre mo-

229 ments beyond the first M expansion terms and produces accurate radiances for practical applica-

230 tions involving strongly forward-peaked scattering phase functions associated with large aerosol,

231 cloud particle, and coastal (turbid) water particles.

232   By accurately representing a majority of the Legendre moments, the δ-M+ algorithm is math-

233 ematically elegant, accurate, reliable, and computationally fast. As in the original δ-M method,

234 the truncation factor of the forward peak is automatically determined by $w_0 f$. The combination

235 of the δ-M method with the single-scattering correction can also be easily accomplished. These

236 advantages make the new δ-M+ method a practical tool that is simple and easy to implement in

237 most radiative transfer models.

238   The δ-M+ algorithm has been implemented in the latest DISORT model available at `http:`

239 `//lllab.phy.stevens.edu/disort/` (Lin et al., 2015) as well as the AccuRT model (Hamre

240 et al., 2017; Stamnes et al., 2017a).

241   Future work, aimed at improvement and extension of the new δ-M+ method, includes 1) finding

242 a possibly better weighting function to replace the simple Gaussian function; 2) testing the perfor-

243 mance of the δ-M+ method when combined with the single-scattering correction and comparing it

14

to the δ-fit and other truncation methods; and 3) applying the δ-M+ method to represent the phase matrix in vector (polarized) radiative transfer models (Min and Duan, 2004; He et al., 2007; Zhai et al., 2009; Cohen et al., 2013; Stamnes et al., 2017b).

References

Arfken, G. B., and H. J. Weber, 1999: Mathematical methods for physicists. AAPT.

Berk, A., P. Conforti, R. Kennett, and T. Perkins, Eds., 2014: *MODTRAN6: a major upgrade of the MODTRAN radiative transfer code*, 9088H, SPIE.

Cohen, D., S. Stamnes, T. Tanikawa, E. Sommersten, J. Stamnes, J. Lotsberg, and K. Stamnes, 2013: Comparison of discrete ordinate and monte carlo simulations of polarized radiative transfer in two coupled slabs with different refractive indices. *Optics express*, **21 (8)**, 9592–9614.

Fournier, G. R., and J. L. Forand, 1994: Analytic phase function for ocean water. *Proc. Ocean Optics XII, SPIE*, **2558**, 194–201.

Hamre, B., S. Stamnes, K. Stamnes, and J. Stamnes, 2017: Accurt: A versatile tool for radiative transfer simulations in the coupled atmosphere-ocean system. *AIP Conference Proceedings*, AIP Publishing, Vol. 1810, 120002.

He, X., D. Pan, Y. Bai, Q. Zhu, and F. Gong, 2007: Vector radiative transfer numerical model of coupled ocean-atmosphere system using matrix-operator method. *Science in China Series D: Earth Sciences*, **50 (3)**, 442–452.

Henyey, L. G., and J. L. Greenstein, 1941: Diffuse radiation in the galaxy. *The Astrophysical Journal*, **93**, 70–83.

Hu, Y.-X., B. Wielicki, B. Lin, G. Gibson, S.-C. Tsay, K. Stamnes, and T. Wong, 2000: δ-fit: A fast and accurate treatment of particle scattering phase functions with weighted singular-value decomposition least-squares fitting. *Journal of Quantitative Spectroscopy and Radiative Transfer*, **65 (4)**, 681–690.

Jin, Z., T. P. Charlock, K. Rutledge, K. Stamnes, and Y. Wang, 2006: Analytical solution of radiative transfer in the coupled atmosphere-ocean system with a rough surface. *Applied optics*, **45 (28)**, 7443–7455.

Joseph, J. H., W. Wiscombe, and J. Weinman, 1976: The delta-eddington approximation for radiative flux transfer. *Journal of the Atmospheric Sciences*, **33 (12)**, 2452–2459.

Kokhanovsky, A. A., and Coauthors, 2010: Benchmark results in vector atmospheric radiative transfer. *Journal of Quantitative Spectroscopy and Radiative Transfer*, **111 (12)**, 1931–1946.

Lin, Z., S. Stamnes, Z. Jin, I. Laszlo, S.-C. Tsay, W. Wiscombe, and K. Stamnes, 2015: Improved discrete ordinate solutions in the presence of an anisotropically reflecting lower boundary: upgrades of the disort computational tool. *Journal of Quantitative Spectroscopy and Radiative Transfer*, **157**, 119–134.

Min, Q., and M. Duan, 2004: A successive order of scattering model for solving vector radiative transfer in the atmosphere. *Journal of Quantitative Spectroscopy and Radiative Transfer*, **87 (3)**, 243–259.

Mitrescu, C., and G. Stephens, 2004: On similarity and scaling of the radiative transfer equation. *Journal of Quantitative Spectroscopy and Radiative Transfer*, **86 (4)**, 387–394.

Nakajima, T., and M. Tanaka, 1988: Algorithms for radiative intensity calculations in moderately thick atmospheres using a truncation approximation. *Journal of Quantitative Spectroscopy and Radiative Transfer*, **40 (1)**, 51–69.

Rozanov, V., A. Rozanov, A. Kokhanovsky, and J. Burrows, 2014: Radiative transfer through terrestrial atmosphere and ocean: software package sciatran. *Journal of Quantitative Spectroscopy and Radiative Transfer*, **133**, 13–71.

Rozanov, V. V., and A. I. Lyapustin, 2010: Similarity of radiative transfer equation: Error analysis of phase function truncation techniques. *Journal of Quantitative Spectroscopy and Radiative Transfer*, **111 (12)**, 1964–1979.

Spurr, R., 2008: Lidort and vlidort: Linearized pseudo-spherical scalar and vector discrete ordinate radiative transfer models for use in remote sensing retrieval problems. *Light Scattering Reviews 3*, Springer, 229–275.

Stamnes, K., and J. J. J. Stamnes, 2016: *Radiative transfer in coupled environmental systems: an introduction to forward and inverse modeling*. John Wiley & Sons.

Stamnes, K., G. E. Thomas, and J. J. Stamnes, 2017a: *Radiative transfer in the atmosphere and ocean*. Cambridge University Press, second edition.

Stamnes, K., S.-C. Tsay, W. Wiscombe, and K. Jayaweera, 1988: Numerically stable algorithm for discrete-ordinate-method radiative transfer in multiple scattering and emitting layered media. *Applied optics*, **27 (12)**, 2502–2509.

Stamnes, K., S.-C. Tsay, W. Wiscombe, and I. Laszlo, 2000: Disort, a general-purpose fortran program for discrete-ordinate-method radiative transfer in scattering and emitting layered me-

17

dia: documentation of methodology. Tech. rep., Tech. rep., Dept. of Physics and Engineering Physics, Stevens Institute of Technology, Hoboken, NJ 07030.

Stamnes, S., S. Ou, Z. Lin, Y. Takano, S. Tsay, K. Liou, and K. Stamnes, 2017b: Polarized radiative transfer of a cirrus cloud consisting of randomly oriented hexagonal ice crystals: The 3×3 approximation for non-spherical particles. *Journal of Quantitative Spectroscopy and Radiative Transfer*, **193**, 57–68.

Takano, Y., and K.-N. Liou, 1989: Solar radiative transfer in cirrus clouds. part i: Single-scattering and optical properties of hexagonal ice crystals. *Journal of the Atmospheric Sciences*, **46 (1)**, 3–19.

Wiscombe, W., 1977: The delta–m method: rapid yet accurate radiative flux calculations for strongly asymmetric phase functions. *Journal of the atmospheric sciences*, **34 (9)**, 1408–1422.

Zhai, P.-W., Y. Hu, C. R. Trepte, and P. L. Lucker, 2009: A vector radiative transfer model for coupled atmosphere and ocean systems based on successive order of scattering method. *Optics express*, **17 (4)**, 2057–2079.

LIST OF TABLES

TABLE 1. Magnitude of the σ and c parameters of the δ-M+ in Figures 3-8.

Figure no.	σ	c
3	10.076	3.528
4	31.700	1.664
5	80.903	1.367
6	180.232	1.016
7	51.749	1.211
8 (100 terms)	162.532	1.208
8 (200 terms)	217.710	1.525

LIST OF FIGURES

FIG. 1. Moments (left) and moment errors (right) of a 20-term δ-M and δ-M+ representation of a H-G scattering phase function with asymmetry factor $g = 0.9$.
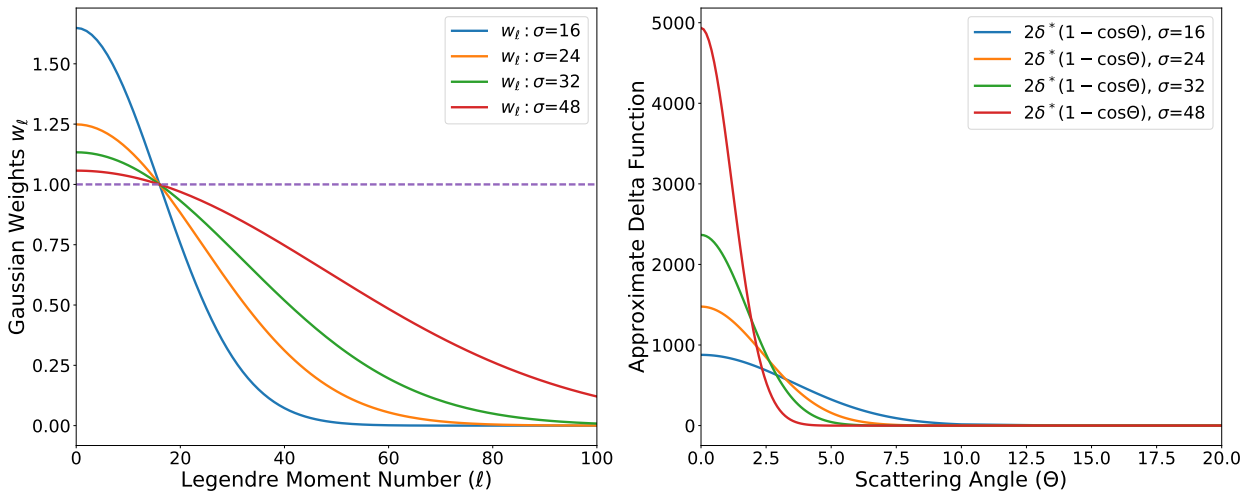
FIG. 2. Gaussian weights and corresponding new approximate delta function $\delta^*(1 - \cos\Theta)$, where c is determined by normalizing $w_{16} = 1$. The horizontal dashed line corresponds to the condition without weighting ($w_\ell = 1$).
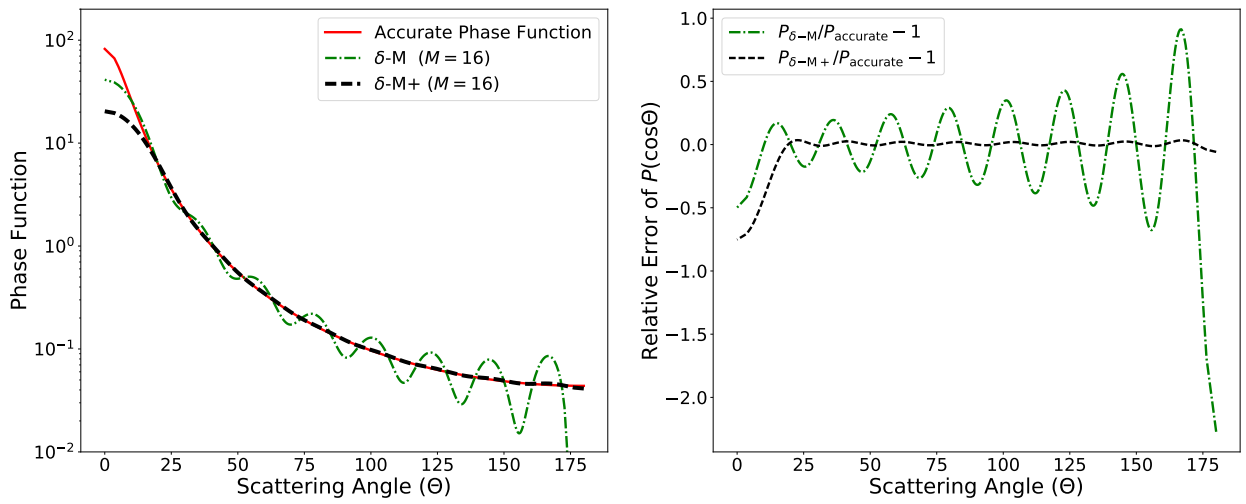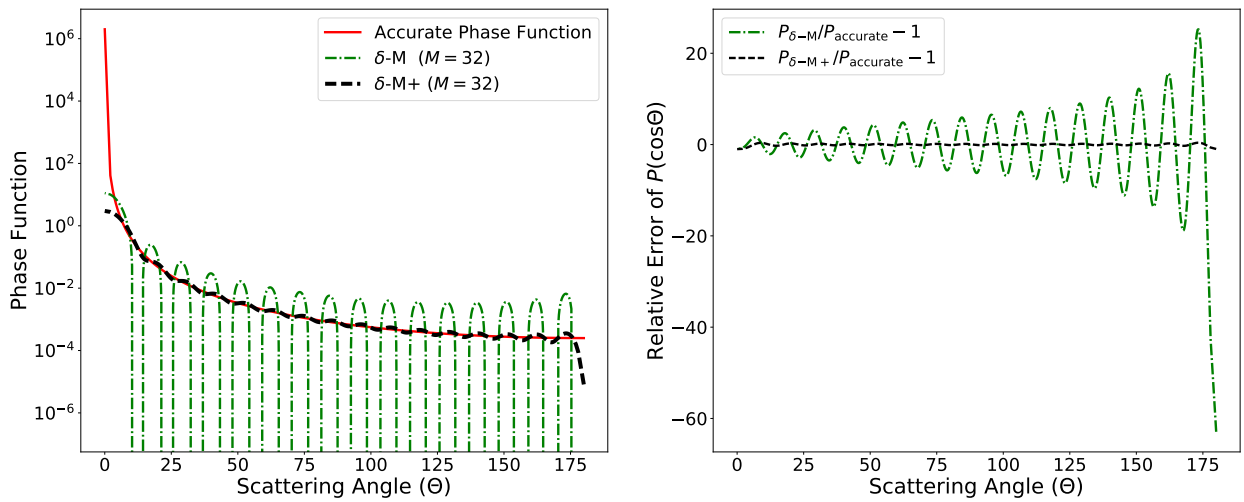
FIG. 3. H-G scattering phase function ($g = 0.85$). 16 terms are used for the Legendre polynomial expansion of the δ-M and the new δ-M+ method. The magnitude of the parameters σ and c are listed in Table 1.
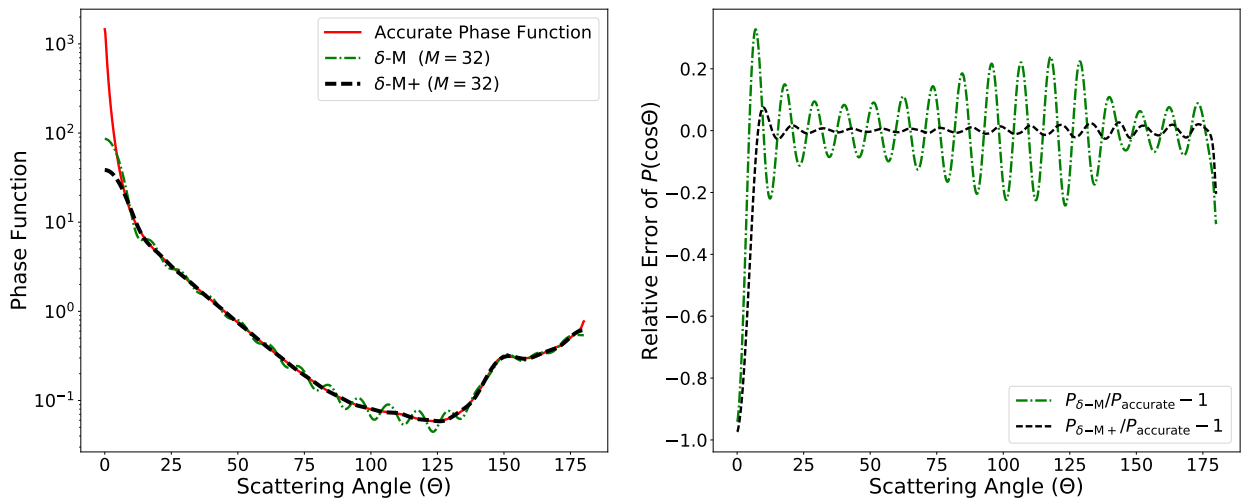
FIG. 4. Kokhanovsky's aerosol scattering phase function. 32 terms are used for the Legendre polynomial expansion of the δ-M and new δ-M+ methods. The magnitude of the parameters σ and c are listed in Table 1.
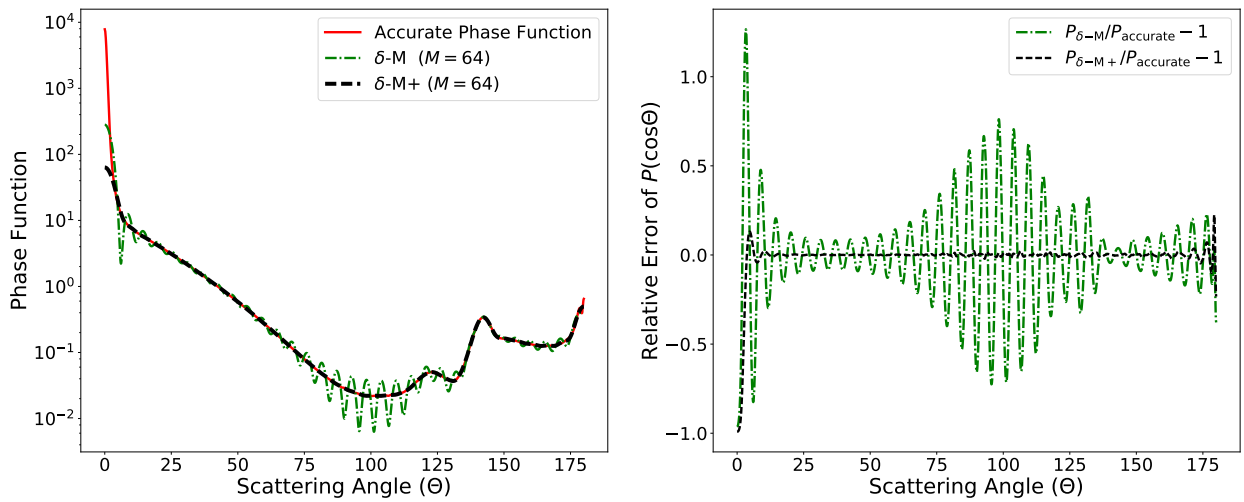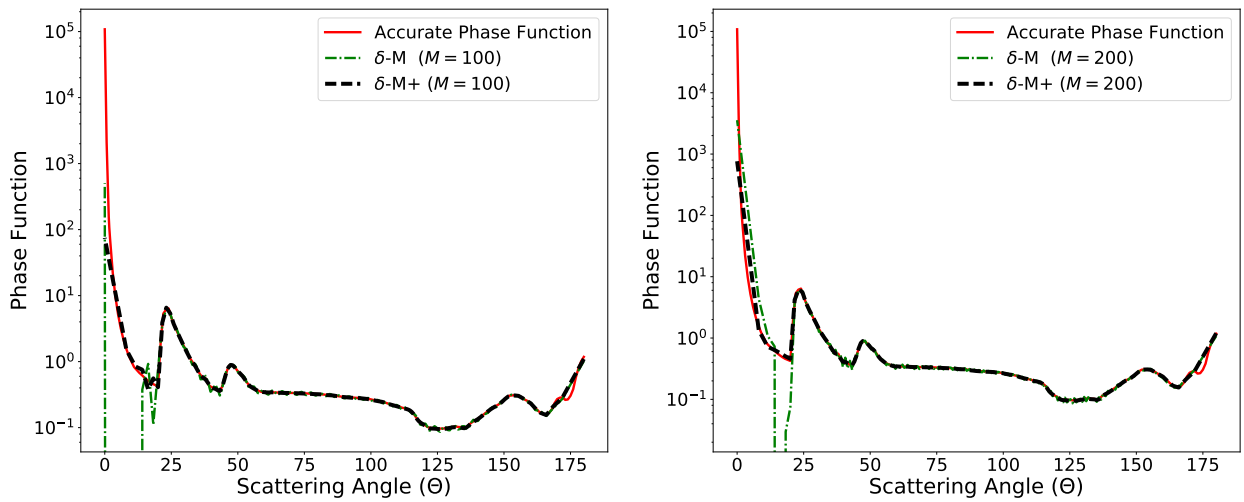
FIG. 5. Kokhanovsky's cloud scattering phase function. 64 terms are used for the Legendre polynomial expansion of the δ-M and new δ-M+ methods. The magnitude of the parameters σ and c are listed in Table 1.

FIG. 6. H-G scattering phase function ($g = 0.999$). 32 terms are used for the Legendre polynomial expansion of the δ-M and the new δ-M+ methods. The magnitude of the parameters σ and c are listed in Table 1.
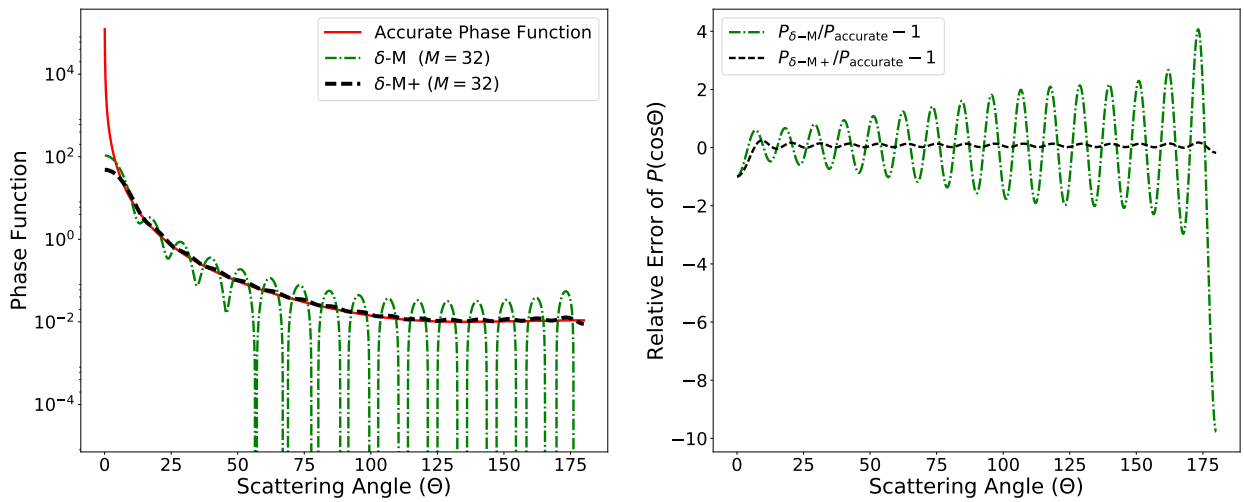
FIG. 7. FF scattering phase function ($m_\mathrm{r} = 1.0686$). 32 terms are used for the Legendre polynomial expansion of the δ-M and the new δ-M+ methods. The magnitude of the parameters σ and c are listed in Table 1.

³⁶² FIG. 8. Ice cloud scattering phase function expanded by 100 terms (left) and 200 terms (right). The magnitude

³⁶³ of the parameters σ and c are listed in Table 1.
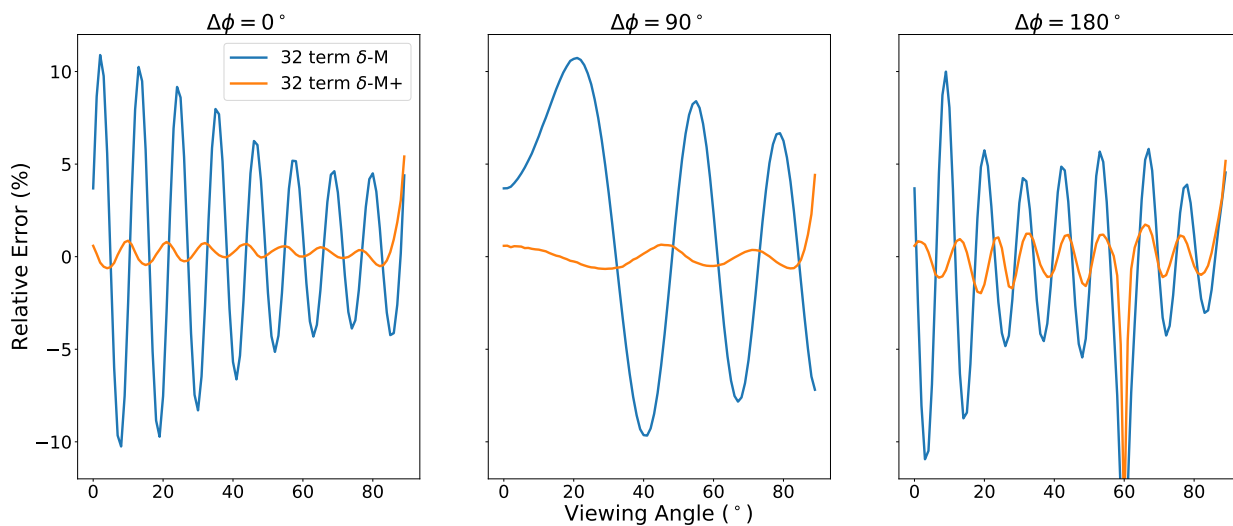
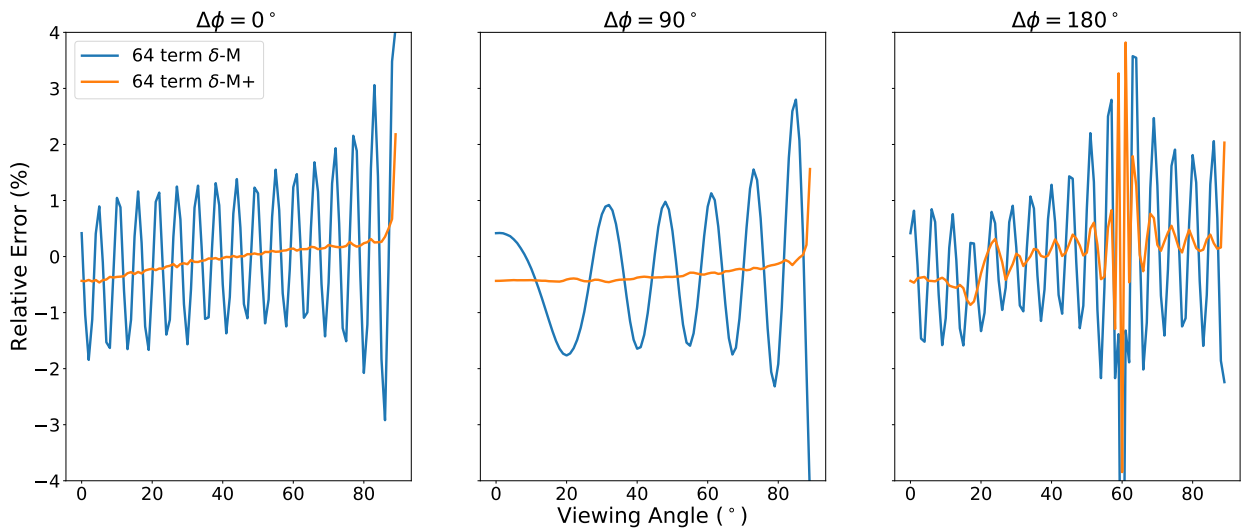FIG. 9. Relative error (%) for the Kokhanovsky aerosol benchmark.

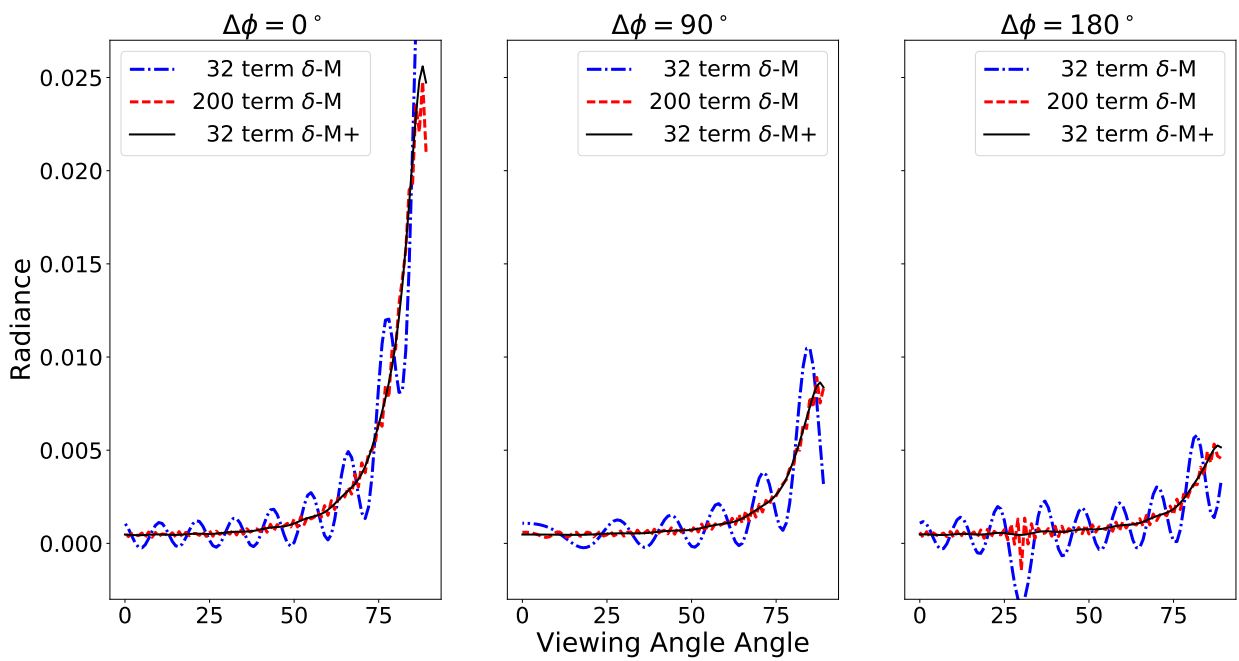FIG. 10. Relative error (%) for the Kokhanovsky cloud benchmark.

FIG. 11. Upward radiance from a homogeneous layer with a FF scattering phase function.